Quartz diorite veins in a peridotite xenolith from Tallante, Spain: implications for reaction and survival of slab-derived SiO_2-oversaturated melt in the upper mantle

By Shoji ARAI,*),†) Yohei SHIMIZU,*) and Fernando GERVILLA**)

(Communicated by Ikuo KUSHIRO, M. J. A., June 10, 2003)

Abstract: We found quartz diorite veins (up to 5 mm thick), composed mainly of plagioclase and quartz, in a plagioclase-bearing spinel lherzolite xenolith in alkali basalt from Tallante, Southern Spain. The quartz diorite veins are coarse-grained, the average grain size being 0.5 mm, and have thin orthopyroxenite rim along olivine wall. Thinner veins free of quartz and composed solely of plagioclase with orthopyroxene selvage are much more common in other xenoliths from Tallante. The involved melt was strongly reactive with olivine to form orthopyroxene, which can protect against further reaction. This suggests how the silica-oversaturated melts, after supplied from downgoing slabs, can move through peridotite and reach the shallow mantle with preserving the silica-oversaturated character. The armor of orthopyroxenite is of vital importance for the melt to keep its silica-oversaturated character within peridotite. Precipitation of orthopyroxene combined with olivine consumption somewhat controls the general chemical trend of adakite. Orthopyroxenite vein network at the expense of olivine is expected to be common as fossil conduits within the mantle wedge. This kind of orthopyroxenite has contributed to Si-enrichment of the mantle wedge.

Key words: Mantle peridotite xenoliths; quartz diorite vein; SiO_2-oversaturated melt; slab; orthopyroxenite; Si-enrichment.

Introduction. Silica-rich melt trapped in the upper mantle peridotite has been recently paid attention by many authors.[1)-3)] It has been interpreted either as slab-derived melt supplied to the mantle wedge[2)] or as a very-small-degree (less than 5%) partial melt of peridotite.[1),3)] Falloon *et al.*,[4)] however, denied the andesitic (silica-oversaturated) character for low-degree anhydrous partial melts of mantle peridotite. Recently crustal emplacement or eruption of silica-rich direct partial melts of subducted slab has been claimed.[5),6)] It is necessary for their reach to the earth's surface to pass through the mantle wedge without losing their SiO_2-oversaturated character through reaction with olivine. However, the evidence for how the SiO_2-oversaturated melts pass through olivine-rich media has not been known to date. Their behavior has been unclear partly because they occur as minute (several microns across) trapped glass[2)] or thin fine-grained veinlets[7)]; that is, they have been possibly quenched not to have sufficiently reacted with surrounding minerals, especially with olivine. In contrast to this, the quartz diorite veins reported here are relatively coarse-grained and has preserved modal quartz, indicating their slower cooling yet preserving a silica-oversaturated character. This has the advantage of examining the reaction of the SiO_2-oversaturated melt with olivine and the survival of SiO_2-oversaturated character, but instead the melt composition is difficult to directly determine because of its slow cooling and coarse-grained character. In this article we describe the quartz diorite veins within the peridotite xenolith from Tallante, Spain, and discuss their implication for the reaction with mantle olivine and the survival of slab-derived SiO_2-oversaturated melts. Detailed mineralogical and geochemical characteristics of the peridotite xenoliths and quartz diorite will be presented in a forthcoming article.

Petrography of the peridotite xenolith. Ultramafic xenoliths, up to 20 cm across, are abundant in alkali basaltic pyroclastics near the village of Tallante, Spain[8)] (Fig. 1). The age of alkali basalt is 2.7 Ma.[9)] The

*) Department of Earth Sciences, Kanazawa University, Kakumamachi, Kanazawa, Ishikawa 920-1192, Japan.
**) Instituto Andaluz de Ciencias de la Tierra, University of Granada-C.S.I.C., Fuentenueva S/N, E-18002, Granada, Spain.
†) Correspondence to: S. Arai.

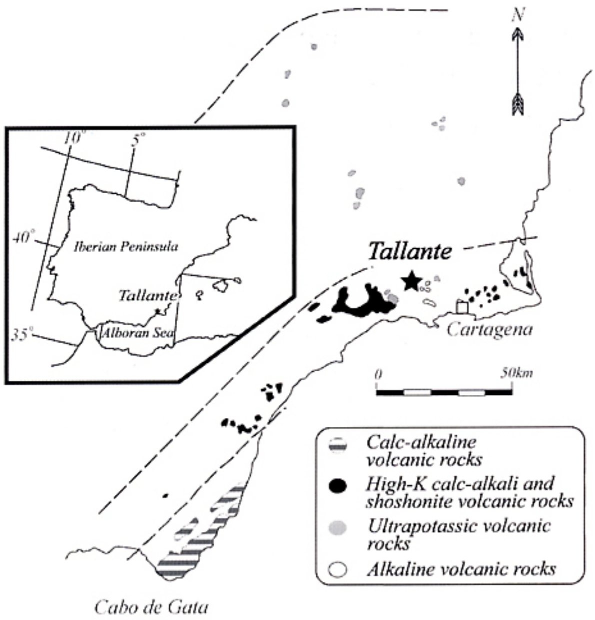

Fig. 1. Locality of the Tallante xenolith and distribution of Miocene calc-alkaline volcanic rocks, Spain (after Fernández-Soler[23]). The calc-alkaline and related magmatism resulted from interaction between the African and European (or Iberia) plates in the Tertiary.[17] Origin of the calc-alkaline magmatisms has been debated.[23)-25] The alkali basaltic magma is the youngest of all magmas in this area.[9),23]

Fig. 2. Photograph of the lherzolite xenolith cut by anastomosing quartz diorite veins (white). Foliation is defined by dark lenticular aggregates of spinel and pyroxenes.

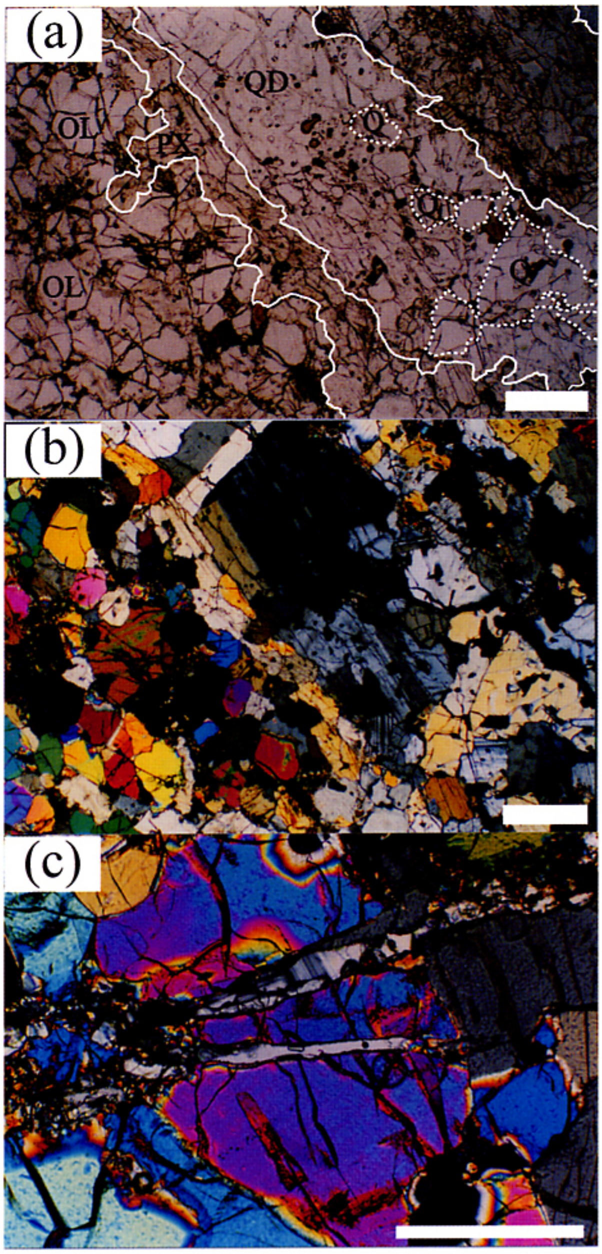

Fig. 3. Photomicrographs of quartz dioritic and related veins in lherzolite from Tallante. (a) A quartz dioritic vein (QD) in lherzolite (Fig. 2). Note the orthopyroxenite lining (PX; highlighted by white solid line) between olivine (OL) and the quartz (Q; highlighted by white dashed line)-plagioclase assemblage. Scale bar, 1 mm. Plane-polarized light. (b) Crossed-polarized light. (c) Thin plagioclase-orthopyroxene vein cutting olivine and primary orthopyroxene (right). Scale bar, 0.5 mm. Crossed-polarized light.

xenoliths are classified into two, Groups I (peridotites) and II (clinopyroxenites and gabbros) in the sense of Frey and Prinz.[10] Composite xenoliths, e.g., xenoliths of peridotite cut by clinopyroxenite or gabbro and of clinopyroxenite enclosing peridotite clasts, are common. The peridotite has equigranular to porphyroclastic textures and is mostly spinel lherzolite to harzburgite, containing less than 10% by volume of clinopyroxene,

Table I. Selected microprobe analyses of minerals of peridotite and quartz diorite

	Host lherzolite				Tonalite vein		
	Ol	Opx	Cpx	Sp	Pl	Opx	Cpx
SiO_2	40.98	55.61	51.40	0.02	54.87	57.43	54.28
TiO_2	0.01	0.10	0.48	0.07	0.00	0.05	0.05
Al_2O_3	0.00	4.44	5.12	57.72	28.94	0.80	0.80
Cr_2O_3	0.06	0.47	0.66	11.38	0.00	0.13	0.08
FeO	9.97	6.25	2.02	9.70	0.08	6.59	4.44
MnO	0.12	0.22	0.06	0.05	0.05	0.10	0.00
MgO	49.50	32.66	16.00	20.16	0.03	34.54	15.66
CaO	0.02	0.48	24.02	0.00	11.60	0.48	25.04
Na_2O	0.01	0.01	0.23	0.05	4.80	0.00	0.18
K_2O	0.03	0.01	0.03	0.03	0.36	0.00	0.02
NiO	0.43	—	—	—	—	—	—
Total	101.12	100.25	100.01	99.17	100.73	100.10	100.56
O	4	6	6	4	8	6	6
Si	0.995	1.913	1.870	0.000	2.461	1.979	1.983
Ti	0.000	0.003	0.013	0.001	0.000	0.001	0.001
Al	0.000	0.180	0.219	1.769	1.530	0.032	0.035
Cr	0.001	0.013	0.019	0.234	0.000	0.003	0.002
Fe*	0.202	0.180	0.061	0.211	0.003	0.190	0.136
Mn	0.002	0.006	0.002	0.001	0.002	0.003	0.000
Mg	1.792	1.675	0.868	0.781	0.002	1.775	0.853
Ca	0.001	0.018	0.936	0.000	0.558	0.018	0.980
Na	0.000	0.001	0.016	0.003	0.418	0.000	0.012
K	0.001	0.000	0.001	0.000	0.021	0.000	0.001
Ni	0.008	—	—	—	—	—	—
Total	3.004	3.988	4.006	3.001	4.995	4.001	4.004
Mg#	0.899	0.903	0.934	0.781		0.903	0.863
Cr#				0.117			
Ca#					0.572		

NOTE: Pl, plagioclase; Opx, orthopyroxene; Cpx, clinopyroxene; Ol, olivine; Sp, chromian spinel.

with or without plagioclase. Peridotites (Group I) are predominant (>80%) over pyroxenites and gabbros (Group II) by volume. Megacrysts of clinopyroxene and kaerusutite are very common.

The peridotite that contains the quartz diorite veinlets is plagioclase-spinel lherzolite with fine-grained lenticular aggregates composed of chromian spinel and pyroxenes (Fig. 2). The aggregates are very similar to those surrounding the spinel-pyroxene symplectite in the Horoman peridotite, Hokkaido, Japan, which has been interpreted as pseudomorphs after pyrope-rich garnet.[11]

Mineral chemistry and petrology of the peridotite host. The host lherzolite contains olivine of $Fo_{89.9}$ and relatively Al-rich spinel of Cr# (= Cr/[Cr+Al] atomic ratio) = 0.12 (Table I). The Tallante peridotite demonstrates systematic variations in mineral chemistry depending on the presence or absence of plagioclase. Olivine is $Fo_{90.5\text{-}91.3}$ in spinel peridotite and $Fo_{89.0\text{-}91.0}$ in plagioclase-spinel one. Cr# of chromian spinel mostly ranges from 0.21 to 0.25 for both types, although its TiO_2 content is clearly different, less than 0.04 wt% in spinel peridotite and 0.1-0.3 wt% in plagioclase-spinel peridotite. Al_2O_3 and Cr_2O_3 contents in pyroxenes are also different between the two types: they tend to be higher in spinel peridotite than in plagioclase-spinel peridotite. Na_2O content in clinopyroxene is slightly higher in spinel peridotite than in plagioclase-spinel one. Interstitial plagioclase is mostly $An_{60\text{-}70}$ but rarely > An_{80} and is very low in K (<Or_1).

Petrography and chemistry of the quartz diorite veins. White veins (up to 5 mm thick) are common in the Tallante peridotite (Fig. 2). They sometimes form a network cutting the foliation of the rocks (Fig. 2). The thicker veins are relatively coarse-grained and are quartz diorite in mode. Quartz, up to 1 mm across, is only in the central part of the veins, and orthopyroxene always intervenes along the olivine-rich wall (Fig. 3a). We found small amounts of zircon, rutile and apatite in quartz diorite. Clinopyroxene, which is anhedral and

Table II. Modal composition and calculated bulk chemical composition of the quartz diorite vein, and composition of adakite and Archean TTG (after Martin, 1999)

Modal composition		Bulk composition			
vol.%		wt.%	Q-diorite	adakite	TTG
plagioclase	73.5	SiO_2	62.9	64.66	69.79
quartz	16.9	TiO_2	0.1	0.51	0.34
orthopyroxene	2.9	Al_2O_3	21.8	16.77	15.56
clinopyroxene	2.7	FeO*	0.4	3.78	2.81
glass	3.7	MnO	0.0	0.08	0.05
others	0.3	MgO	1.5	2.20	1.18
		CaO	9.6	5.00	3.19
		Na_2O	3.6	4.09	4.88
		K_2O	0.3	1.72	1.76
		P_2O_5	0.1	0.17	0.13
Total	100.0	Total	100.3	98.98	99.69

FeO*, total iron as FeO. See text for explanation.

coarse (up to 2 mm across), is in contact with quartz and poikilitically encloses plagioclase laths. Plagioclase is slightly zoned, and orthopyroxene is free from clinopyroxene lamellae. K-feldspars are absent. Small amounts of hydrous minerals (pargasite and phlogopite) are distributed in adjacent peridotite wall: phlogopite forms especially around primary chromian spinel. Thinner veins are free from quartz and are mainly composed of plagioclase and orthopyroxene (Fig. 3c).

We estimate the modal composition of the quartz diorite veins by measuring the area of each phase on photomicrographs. Pyroxenes lining the olivine wall (Fig. 3ab) are excluded from the treatment. Plagioclase and quartz occupy more than 90% of the vein in volume (Table II). The rock is quartz diorite according to the nomenclature of Streckeisen.[12]

Plagioclase in the quartz diorite veins (Table I) is slightly less calcic than interstitial one and shows normal zoning, from An_{54-61} to An_{47-52} from the core outward. Its K content is negatively correlated with An, ranging from $Or_{1.5}$ to $Or_{4.1}$. Orthopyroxene in the veins is as magnesian as but is distinctly lower in CaO (0.6 to 0.2 wt%), Al_2O_3 (2 to 0.8 wt%) and Cr_2O_3 (0.2 wt% to nil) than that in the peridotite (Table I). Clinopyroxene in quartz diorite is diopside with high Mg# (= Mg/(Mg + total Fe) atomic ratio), ca. 0.89, and low contents of TiO_2 (0.1-0.2 wt%), Al_2O_3 (0.7-0.8 wt%) and Cr_2O_3 (<0.1 wt%) (Table I). Both phlogopite and hornblende are low in TiO_2, < 1.8 wt% and < 1 wt%, respectively. The olivine wall apparently has no chemical gradient toward the vein: the Fo content is constantly around 90. A chemical gradient, however, does exist within the orthopyroxene selvage; its Mg# decreases from around 0.90 to 0.87 inward over 1 to 2 mm.

We calculated the bulk composition of the quartz diorite based on the modal composition above and averaged composition of each phase (Table II). The rock is rich in Al_2O_3 and CaO relative to the averaged adakite and Archean TTG (tonalite, trondhjemite and granodiorite) (Table II)[13] due to high content of relatively Ca-rich plagioclase (Tables I & II).

Discussion. The quartz diorite is rich in Al and Ca, being different in composition either from averaged adakites and Archean TTG, possible slab melts, (Table II)[13] or from high-pressure experimental melts of basalts (or eclogites), an analogue of slab melts.[14] The melt involved in the formation of quartz diorite within the Tallante peridotite was silica-oversaturated and was strongly reactive with olivine to produce orthopyroxene. This is different from the behavior of mantle partial melt which tends to be oversaturated with olivine with a pressure decrease[15] and to form dunite with consumption of orthopyroxene.[16] The melt was most probably derived from melting of crustal materials, the descending or sinking slab beneath the Betic area[17] in spite of the chemical difference from possible slab melts. We interpret that the Tallante quartz diorite is not frozen melt but is plagioclase-cumulative.

The mode of occurrence of the quartz dioritic veins strongly suggests that the silica-oversaturated melt changes its composition basically by a reaction, olivine digestion combined with orthopyroxene precipitation. It can preserve its original character (e.g., silica oversaturation and low Cr) to some extent only if continuously armored by the reaction product, orthopyroxene, from ambient peridotite. Larger melt/olivine ratio

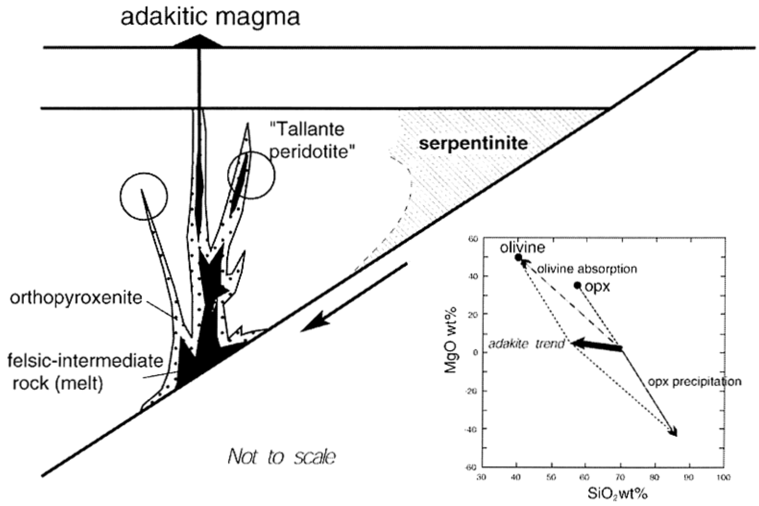

Fig. 4. Schematic profile of the mantle wedge to show the behavior of silica-oversaturated melt derived from the slab. Orthopyroxene is precipitated at the expense of olivine. Note that the reaction is prominent in the middle of mantle wedge due to high temperature.[26] Inset is to explain the compositional variation of adakite by orthopyroxene precipitation combined with olivine absorption. The adakite trend is after Defant and Kepezhinskas.[6]

and fissure flow mechanism are favorable for preservation of the original character. This means that the Tallante quartz dioritic melt has left larger amount of orthopyroxenite at the expense of olivine below, because the host peridotite was derived from the shallowest part of the upper mantle of plagioclase-lherzolite stability field, at < 1GPa.[18] The melt which produced the quartz diorite veins had been in equilibrium with peridotite wall through orthopyroxene lining in terms of Mg-Fe distribution due to slow cooling since no appreciable chemical gradient for Mg# is found within the peridotite part (Fig. 2). The inward fractional crystallization of the melt during subsequent cooling had produced a steep and narrow chemical gradient across the thin orthopyroxene selvage (Mg#, 0.90 to 0.87).

The geochemical characteristics of the involved silica-rich melt are difficult to estimate as mentioned above. The principles of behavior of silica-oversaturated melt within the mantle peridotite can be deduced from the Tallante example. The compositional trend of high-Mg# adakites[6),19)] is apparently controlled by subtraction of orthopyroxene combined with olivine addition (Fig. 4). Adakitic or other silica-rich melts derived from slab therefore necessarily leave orthopyroxene-rich rocks at the expense of olivine as fossil melt conduits within the mantle wedge *en route* to the surface (Fig. 4).

A different kind of secondary orthopyroxene also replacing olivine has been recently reported from several sub-arc mantle peridotites.[20),21)] It replaces olivine commonly with complicated boundaries and is free from associated minerals. We suggest that the metasomatic agent for such kind of secondary orthopyroxene was not silicate melts but was aqueous fluids enriched with silica.

The frequent occurrence of the secondary orthopyroxenes in the arc-derived mantle peridotites suggests that they are common in mantle wedge as a result of silica enrichment by both melts and by fluids from the subducted slab.[22] Orthopyroxenite network (or parallel banding if extensively deformed) is common within mantle wedge as trails of silica-rich metasomatic agents from subducted slab.

Acknowledgements. We are very grateful to Prof. I. Kushiro, M. J. A., for his comments and discussion. We are indebted to Ms. M. Kida and Ms. C. Tanaka for their assistance in the field, and to Dr. K. Kadoshima, Dr. H. Watanabe and Mr. A. Tsune for their help in microprobe and modal analyses. Discussion with Dr. T. Morishita was helpful.

References

1) Schiano, P., and Clocchiatti, R. (1994) Nature **368**, 621-624.
2) Schiano, P., Clocchiatti, R., Shimizu, N., Maury, R. C., Jochum, K. P., and Hofmann, A. W. (1995) Nature **377**, 595-600.
3) Hirschmann, M. M., Barker, M. B., and Stolper, E. M. (1998) Geochim. Cosmochim. Acta **62**, 883-902.
4) Falloon, T. J., Green, D. H., O'Neill, H. St. C., and Hibberson,

W. O. (1997) Earth Planet. Sci. Lett. **152**, 149-162.
5) Defant, M. J., and Drummond, M. S. (1990) Nature **347**, 662-664.
6) Defant, M. J., and Kepezhinskas, P. (2001) EOS **82**, 65, 68-69.
7) Kepezhinskas, P. K., Defant, M. J., and Drummond, M. S. (1995) J. Petrol. **36**, 1505-1527.
8) Capedri, S., Venturelli, G., Savioli-Mariani, E., Crawford, A. J., and Barbieri, M. (1989) Eur. J. Mineral. **1**, 685-699.
9) Bellon, H., Bordet, P., and Montenat, C. (1983) Bull. Soc. Géol. France **25**, 205-217.
10) Frey, F. A., and Prinz, M. (1978) Earth Planet. Sci. Lett. **38**, 129-176.
11) Takahashi, N., and Arai, S. (1989) Sci. Rep. Inst. Geosci. Univ. Tsukuba **B10**, 45-55.
12) Streckeisen, A. (1976) Earth Sci. Rev. **12**, 1-33.
13) Martin, H. (1999) Lithos **46**, 411-429.
14) Rapp, R. P., and Watson, E. B. (1995) J. Petrol. **36**, 891-931.
15) Kushiro, I. (1969) Amer. J. Sci. **267-A**, 269-294.
16) Quick, J. E. (1981) Contrib. Mineral. Petrol. **77**, 185-194.
17) Blanco, M. J., and Spakman, W. (1993) Tectonophys. **221**, 13-34.
18) Kushiro, I., and Yoder, H. S., Jr. (1966) J. Petrol. **7**, 337-362.
19) Kay, R. W. (1978) J. Volcanol. Geotherm. Res. **4**, 117-132.
20) Smith, D., Riter, J. C. A., and Mertzman, S. A. (1999) Earth Planet. Sci. Lett. **167**, 347-356.
21) Arai, S., and Kida, M. (2000) Island Arc **9**, 458-471.
22) Kelemen, P. B., Hart, S. R., and Bernstein, S. (1998) Earth Planet. Sci. Lett. **164**, 387-406.
23) Fernández-Soler, J. M. (1996) El Volcanismo Calco-Alcalino en el Parque Natural de Cabo de Gata-Níjar (Almería) Estudio Volcanológico y Petrológico. Sociedad Almeriense de Historia Natural, Almería, Spain, pp. 1-295.
24) Zeck, H. P. (1996) Tectonophys. **254**, 1-16.
25) Turner, S. P., Platt, J. P., George, R. M. M., Kelly, S. P., Pearson, D. G., and Nowell, G. M. (1999) J. Petrol. **40**, 1011-1036.
26) Tatsumi, Y., Sakuyama, M., Fukuyama, H., and Kushiro, I. (1983) J. Geophys. Res. **88**, 5815-5825.